

Depolarization properties of the femtosecond supercontinuum generated in condensed media

R. Sai Santosh Kumar, K. L. N. Deepak, and D. Narayana Rao*
School of Physics, University of Hyderabad, Hyderabad 500 046, India
 (Received 18 June 2008; published 16 October 2008)

In this paper, we present a study of depolarization of a supercontinuum across its spectral range as a function of the femtosecond laser pump intensity for an anisotropic crystalline condensed medium, potassium-dihydrogen-phosphate (KDP) crystal, and compare our results with commonly used supercontinuum generation (SCG) materials, namely borosilicate glass Schott (BK-7) glass (representing isotropic amorphous condensed media) and BaF₂ (isotropic crystalline condensed media). Our results show that at higher input powers, depolarization in the continuum increases for BK-7, BaF₂, and along the direction of the optic axis of the KDP crystal. However, in the case of KDP crystal, we observe that the depolarization properties are strongly dependent on (i) the plane of polarization of incident light and (ii) the orientation of the crystal with respect to the incident light. Our studies also confirm that one can achieve SCG in a KDP crystal that maintains the same state of input polarization even at high input intensities when proper orientation of the crystal is used.

DOI: [10.1103/PhysRevA.78.043818](https://doi.org/10.1103/PhysRevA.78.043818)

PACS number(s): 42.25.Ja, 42.70.Mp, 42.65.Jx, 42.65.Re

I. INTRODUCTION

When focused into a transparent medium, the interaction of intense ultrashort optical pulses with the medium becomes strongly nonlinear. The temporal, spatial, and spectral properties of an ultrashort pulse undergo modification when it propagates through such a medium, resulting in the generation of a spectrally broad white light termed as supercontinuum (SC) [1,2]. The self-transformation of the pulse shape and spectral broadening are the result of strong nonlinear-optical interaction of the light field with the medium, which takes place in the conditions of high localization of the radiation both in space and time. Supercontinuum generation (SCG) is one of the most intriguing and spectacular phenomena associated with the propagation of high-intensity ultrashort laser pulses through gases, liquids, and solids. The power threshold for continuum generation is determined to be coinciding with the calculated critical power for self-focusing [3]. When the laser power incident on a medium exceeds the critical power $P_{cr}=3.77\lambda_0^2/8\pi n_0 n_2$ [4] for self-focusing, a catastrophic collapse of laser pulse occurs at a finite distance. Here, the linear and nonlinear refractive indices of the medium are denoted by n_0 and n_2 , respectively, and λ_0 is the wavelength of the laser in vacuum. The spectral broadening is widely understood to be the contribution of several nonlinear processes, acting concomitantly, that include (i) self-phase modulation, (ii) optical “shock wave” formation due to self-steepening, (iii) space-time focusing, and (iv) plasma generation by multiphoton ionization [5]. Based on recent experimental and theoretical results [6–8], it can also be assumed that different spectral components of the SC are generated at different positions along the propagation pathway of the pulse through the medium. The pump laser during its propagation gets self-focused and the leading edge creates multiphoton ionization (MPI) and plasma leading to broadening around the laser line. This MPI and plasma de-

focus the trailing edge of the laser pulse. On further propagation in the medium, subsequent space-time focusing and self-steepening create a steep back edge, resulting in the appearance of a broad blue wing in the SC spectrum [5,7,8]. Theoretical studies have shown that besides the plasma-induced frequency blueshift, the linear chromatic dispersion plays an important role in determining the achievable spectral extent of the supercontinuum as well [9]. With its high spatial coherence, good polarization properties, spectral brightness, and high peak intensities enabling strong light-matter interaction in the nonlinear regime [1], SC has found a myriad of applications as an ideal broadband ultrafast light source. Major applications include femtosecond time-resolved spectroscopy, optical pulse compression for generation of ultrashort pulses, a seed pulse of an optical parametric amplifier, optical frequency metrology, two-photon absorption spectroscopy, biomedical applications [10–15].

In the past two decades, much research has gone into the generation of SC in various materials like microstructured fibers, photonic band-gap crystal fiber (PCF), birefringent fibers, BaF₂ crystal, and sapphire [2,16–20]. Earlier, we reported the generation of broadband white light in a quadratic nonlinear medium, KDP crystal, where we have made use of the second-harmonic generation in tandem with SCG in the KDP crystal [21]. By employing SCG and sum frequency generation (SFG) in tandem, the tunability of SCG in the shorter wavelength regime (i.e., <400 nm) was achieved along with the generation of ultrabroadband SCG with suitable orientation of the crystal [22].

Apart from generating spectrally broad SC, a prior knowledge of the polarization properties of SCG is of utmost importance as continuum with stable polarization properties plays an important role in many of the spectroscopic applications. Thus, in this scenario, research in materials for generating SCG with stable polarization properties has gained precedence over generating SCG with ultrabroad spectral width. The general assumption is that the generated supercontinuum (SC) follows the state of polarization of the input pump pulse [1]. However, a distinct degree of the degradation of polarization (depolarization) of SC generated in isotropic materials is known to set in with an increase in the

*Author to whom correspondence should be addressed: dnrsp@uohyd.ernet.in; Fax: +91-40-23011230.

input intensities owing to the onset of multiphoton-induced free-electron generation, which also corresponds to the onset of asymmetry in white light spectra [23]. For linear input polarization, the SC spectrum was found to show strong depolarization around the input wavelength, while the preservation of the input polarization is pronounced toward the blue spectral region [24]. As many nonlinear optical experiments require higher intensities for the continuum, it becomes a necessity to pump at higher intensities. While doing so, the medium generating the continuum gets damaged, and to avoid such damages, it is commonly practiced to rotate or translate the medium. Such rotations or translations were assumed to produce stable intensity and do not affect the continuum properties [25,26]. However, the polarization of SC is ascertained to depend strongly on the orientation of crystalline media (like sapphire) with respect to the plane of polarization of the pump light [27], thus contradicting the earlier assumption.

From the available literature pertaining to the study of polarization properties of SCG, most of the studies are carried out in either of the following ways: (a) an integrated fashion, i.e., over the entire spectrum [1,28,29]; (b) in a very narrow spectral range but covering the entire SC spectra [23,27]. Recently, interest in the study of the spectral dependence of the polarization properties has gained precedence over the integrated measurements. In this regard, extensive work on the polarization properties of SCG in cubic materials like CaF_2 and sapphire crystal were reported [24,30]. Polarization of SC generated in CaF_2 plate was shown to depend strongly on the orientation of the crystal with respect to the plane of polarization of the pump light. The intensity modulation of the broad blueshifted wing of SC against crystal rotation for both the polarizations parallel and orthogonal to the polarization of the pump beam was observed with both CaF_2 and sapphire [30]. This study [30] was performed with input power that corresponds to a maximum of $10P_{\text{cr}}$ for CaF_2 ($P_{\text{cr}}=2$ MW) where a stable single filament could be obtained. As an increase in input power results in the increase of input peak intensities, one would expect an increase in the degree of depolarization. This demands the study of polarization properties of the SC at high input powers.

In light of the prevailing knowledge of the above-mentioned studies on polarization properties of SCG, we performed studies of depolarization (defined as loss of input polarization) of SC at a very high input intensity in KDP crystal. Our preliminary results were presented elsewhere [31], in which we demonstrated the use of noncentrosymmetry crystal in controlling the polarization properties of SC. In this paper, we present our detailed systematic study of depolarization of SCG across its spectral range with respect to an increase in input powers from $\sim 50P_{\text{cr}}$ to $2500P_{\text{cr}}$ for three classes of popular SCG materials: (a) BK-7 glass ($P_{\text{cr}} \sim 2.5$ MW) representing isotropic amorphous condensed media, (b) BaF_2 ($P_{\text{cr}} \sim 3.4$ MW) isotropic crystalline condensed media, and (c) KDP crystal ($P_{\text{cr}} \sim 2.8$ MW for a z -cut crystal) anisotropic crystalline condensed media. Our results at high input peak powers show that there is complete depolarization of SCG in all media. However, in the case of KDP crystal, we observe that the depolarization properties are dependent on (i) the plane of polarization of incident light, and

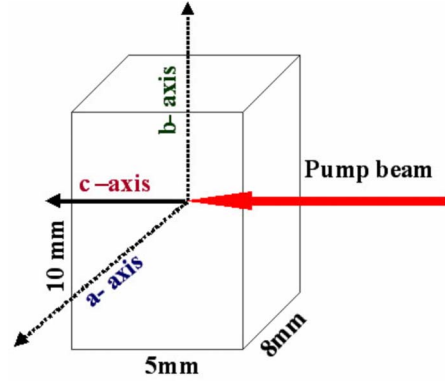


FIG. 1. (Color online) Position of the crystal used in the study.

(ii) the incident orientation of the crystal. Our study also confirms that one can achieve SCG that maintains the same state of input polarization even at high input intensities with appropriate orientation of the crystal. We also present the integrated spectral intensities measurements to supplement our spectral-dependent data.

II. EXPERIMENTAL DETAILS

The experiments are performed with a Ti:sapphire system (MaiTai+Spitfire, Spectra Physics Inc.), delivering 1 mJ, 100 fs duration laser pulses at 800 nm and 1 kHz repetition rate. The input polarization is p -polarized (extinction ratio $< 10^{-3}$). The SC is generated by focusing the 800 nm pulse into three different media using a focusing lens of focal length $f=300$ mm. The media considered for the study are (i) a z -cut KDP crystal with dimensions $10 \times 8 \times 5$ mm³, (ii) 1.5-cm-thick BK-7 glass, and (iii) 10 mm BaF_2 crystal (EK-SLPA, Lithuania) cut for (001) orientation. While comparing the SCG in these three media, an input beam is considered to be polarized parallel to the (100) axis of the crystal and propagating along the (001) axis of the KDP and BaF_2 crystals as shown in Fig. 1. The calculated beam waist, taking a Gaussian beam approximation, at the focal point in vacuum was ~ 50 μm . The face of the sample was always placed 2 cm away before the focus point to avoid any laser-induced damage. The incident average power used for the study was varied from 10 to 600 mW corresponding to a maximum peak power variation of ~ 0.1 – 6.0 GW (~ 50 – $2500P_{\text{cr}}$ for BK-7 glass). This accounts for peak intensity of a maximum $\sim 15 \times 10^{12}$ W/cm² on the front face of the sample. The calculations of the peak powers and peak intensities were performed assuming the Gaussian beam profile for the incident pulse. The spectra of continuum are recorded using a fiber coupled spectrometer (Ocean Optics USB2000) after collimation and suppressing fundamental by an ir filter, thus limiting our study of SC to the visible region (400–750 nm). The detector used in the spectrometer was a silicon charge coupled device that has a range from 350 to 800 nm with maximum sensitivity at 500 nm. Beyond 750 nm, there is a monotonic decrease in the detector sensitivity. The fiber used for collection has excellent transmission for the range

300–900 nm. The polarization of the SC is analyzed with Glan-Thomson polarizer (extinction ratio $\sim 10^5$, Thorlabs). Care has been taken to see that the SC entering the Glan polarizer is well collimated. Neutral density filters with known absorption spectra in the region were used to collect the continuum spectra obtained at high input powers. Taking into account the absorption spectra of the filters used, the resultant spectra thus obtained are corrected and presented in this paper. For the integrated intensity measurements, the SC in both parallel (I_{par}) and perpendicular position (I_{orth}) are performed by focusing onto a photodetector (FND100) after suppressing the fundamental using a 750 nm low pass filter (Thorlabs). Different orientations of the crystal presented in the study were confirmed by x-ray piezo-goniometer (Rigaku, Japan).

III. RESULTS AND DISCUSSION

A. Depolarization properties of SCG from BK-7, BaF₂, and KDP

In this paper, we discuss our results on the degree of depolarization that sets in the supercontinuum generated at high input powers in BK-7, BaF₂, and KDP. To compare the continuum generated in these media, we used the following methodology [24]. The polarization of the SC was examined by the transmitted SC spectra through the analyzer at perpendicular [$I_{\text{orth}}(\lambda)$] and at parallel orientations [$I_{\text{par}}(\lambda)$] of the Glan polarizer with respect to the input polarization as a function of the wavelength (λ). We define the ratio of $I_{\text{par}}(\lambda)$ to $I_{\text{orth}}(\lambda)$ as the polarization ratio [$\rho(\lambda)$]. Thus, the larger the observed changes of the SC polarization (depolarization), the smaller the resulting values of ρ , and hence the input polarization retained in the process of continuum generation can be presented by the polarization ratio. We define the integrated polarization ratio (ρ_{int}) as the ratio of integrated spectral intensity (over the entire continuum) $I_{\text{par}}^{\text{int}}$ to $I_{\text{orth}}^{\text{int}}$. While comparing the SC in the three media, we mention the different peak powers in multiples of critical power for self-focusing (P_{cr}) for BK-7 glass.

Figure 2 shows the typical SC spectra of the different media under consideration for an input power of 350 mW, corresponding to $\sim 1400P_{\text{cr}}$ and a peak intensity of 8×10^{12} W/cm². The broad blue pedestal at such a high input power is mainly because, with an increase of the incident power, apart from the Kerr effect, free electrons that are generated due to multiphoton ionization (MPI) also begin to contribute to spectral broadening of the fundamental input pulse. In the high power regime, the time variation of the refractive index due to these free electrons leads to asymmetric spectral broadening that is blueshifted while the space variation of the refractive index gives rise to defocusing [32]. The free electrons generated due to MPI give rise to plasma that induces a spectral shift. This onset of plasma-induced free-electron generation has been suggested as the reason for the polarization degradation [23]. Thus, one would expect the polarization of the SCG to get degraded to a large extent at these higher intensities. This is very apparent in Fig. 3, which shows the variation of ρ_{int} with an increase in input power, where for the input power corresponding to $1400P_{\text{cr}}$,

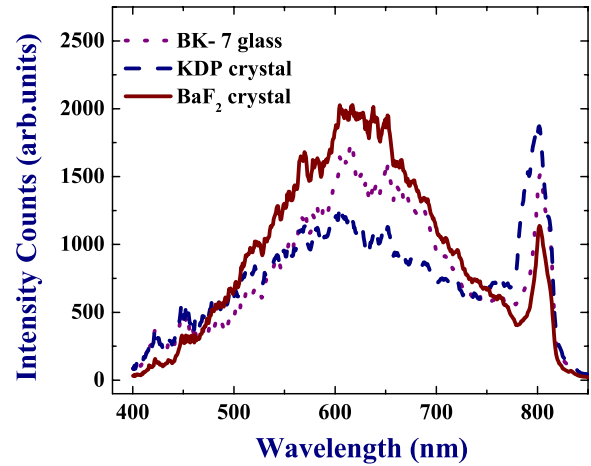


FIG. 2. (Color online) Supercontinuum spectra of transparent media under study: BK-7 glass, a z-cut KDP crystal positioned as in Fig. 1 and BaF₂ crystal.

the integrated polarization ratio is very low, indicating maximum depolarization.

From Fig. 3, we observe that as the input powers go beyond $250P_{\text{cr}}$, there is a dramatic reduction in the ρ_{int} of the SC for all the three media, and beyond $500P_{\text{cr}}$ the ρ_{int} remains a minimum indicating that the SC generated for input powers $>500P_{\text{cr}}$ for any media is mostly depolarized. A closer look into the plot also gives an indication that for lower input powers, SC from BK-7 glass (amorphous) has better ρ_{int} when compared to that of the other two crystalline media. This observation is in agreement with that of an earlier work by Midorikawa *et al.* [27], which reports that there is a self-induced polarization change of the SC in crystalline media that are optically isotropic and do not show linear birefringence in an ordinary optical field. Though the KDP crystal is an anisotropic media, in this case we can safely assume it to be isotropic as the SC is generated along its c axis, which coincides with its optic axis. Thus, at first glance one would get the impression that for lower input powers the SCG in BK-7 glass has least depolarization, although with an

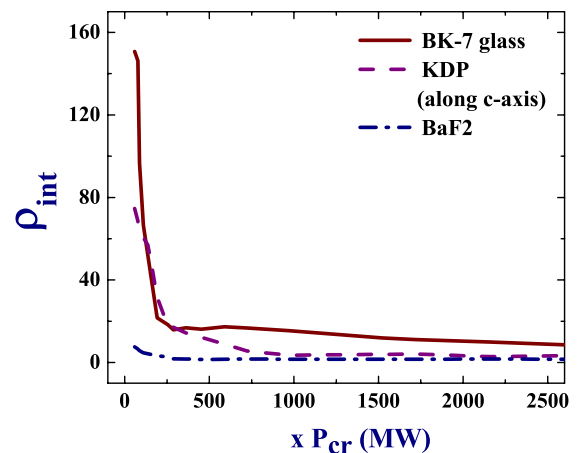


FIG. 3. (Color online) Plot of integrated polarization ratio [ρ_{int}] of the SC from the different media with an increase in the input power in terms of the critical power (P_{cr}).

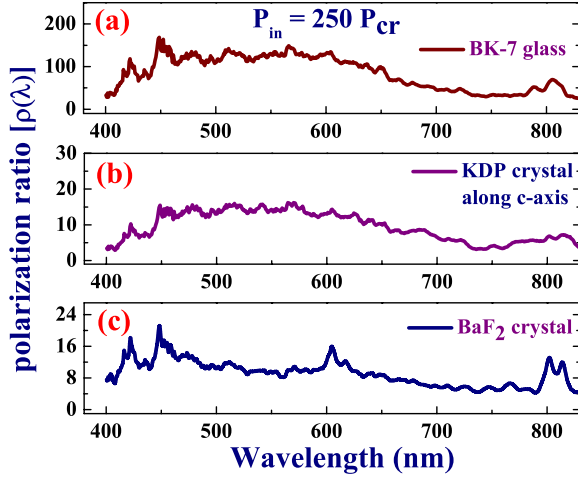


FIG. 4. (Color online) Spectral polarization ratio $[\rho(\lambda)]$ of the SC at $P_{in}=250P_{cr}$.

increase in input power, all media generate depolarized continua. As the data presented above are the integrated intensity over the entire continuum, we carried out experiments to see the depolarization at different regions of the spectrum using a spectrometer and the Glan polarizer.

Figure 4 shows the polarization ratio $[\rho(\lambda)]$ of the SC across the spectra under consideration at a very low input power ($P_{in} \sim 0.6$ GW, corresponding to $\sim 250P_{cr}$ and $I_{in} \sim 1.5 \times 10^{12}$ W/cm²). The most striking observation from the figure is that the $\rho(\lambda)$ for SC of any of the three media is not the same across the continuum spectrum. We find the small peak at 800 nm (residual of fundamental) is surrounded by a pronounced SC depolarization. In contrast, the blue region of the SC (450–750 nm) shows less depolarization, and ρ rises toward the blue edge of the spectrum. The observed phenomenon can be rationalized by considering that since different spectral components of the SC are generated at different positions along the propagation pathway of the pulse through the medium, the fate of the polarization of each component is determined by its corresponding nonlinear anisotropic birefringence (NAB) and its interaction length in the SC filament. Because of the input power being several times the critical power of self-focusing, the input pulse effectively undergoes catastrophic collapse resulting in space-time focusing and self-steepening forming an “optical shock” wave inside the medium at a certain distance from the filament starting point [5]. The multiphoton absorption and plasma defocusing weaken the trailing edge of the pulse. Therefore, the effective length of interaction of the SC spectrum components, with the most intense part of the pulse at 800 nm, decreases toward the blue part of the spectrum. Thus a more pronounced depolarization is observed for the SC spectrum around the input wavelength, while minor depolarization occurs in the blue wing.

Comparing $\rho(\lambda)$ for the different media, we observe that BK-7 glass has a better ratio compared to that of KDP and BaF₂ crystal for lower input powers. In the case of BK-7 glass, the value of ρ in the blue region is as high as ~ 150 when compared to those of KDP and BaF₂ crystal, which have values less than 25. The depolarization of SC from

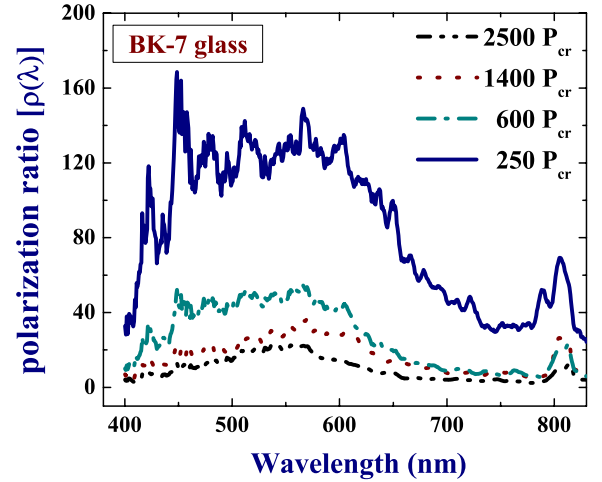


FIG. 5. (Color online) $\rho(\lambda)$ of the SC from BK-7 glass with an increase in the input power in terms of the critical power (P_{cr}).

BK-7 glass is lower presumably because, owing to its amorphous nature, the effect of NAB is minimal at lower intensities and the depolarization is mainly because of the interaction of the input pulse with the plasma [23]. However, we find further depolarization in the case of the crystalline media like KDP and BaF₂ in addition to the effect of plasma, as there is a substantial contribution of a self-induced nonlinear polarization change due to the effect of NAB because of the intrinsic anisotropic $\chi^{(3)}$ tensor (i.e., it contains some non-zero off-diagonal elements) [24]. Thus, it can be concluded that for lower input powers, the material representing amorphous isotropic media has a better polarization ratio compared to the crystalline media. On the other hand, at such lower input powers, the blue pedestal in the SC spectra is not intense enough and that could prove to be a limitation for the applications requiring a spectrally bright SC source.

BK-7 glass, which shows good $\rho(\lambda)$ at low input powers, nevertheless experiences gradual reduction with the increase in input power. Figure 5 shows the variation of the $\rho(\lambda)$ for input peak powers of 250, 600, 1400, and 2500 P_{cr} that corresponds to the input intensities of 1.5, 3.5, 6.3, and 15×10^{12} W/cm², respectively. For input of 2500 P_{cr} , we observe that the overall ρ is less than 10 throughout the blue pedestal of the SC indicating maximum depolarization. This is because, even though BK-7 is an optically isotropic glass, at high input powers it is known to undergo a self-induced polarization change because of the transient nonlinear birefringence induced by the incident laser beam itself inside the sample [33]. On the other hand, KDP and BaF₂ crystals show rapid depolarization compared to BK-7 at higher input powers as shown in Figs. 6 and 7, respectively. For input of 2500 P_{cr} , we observe that the overall ρ is less than 5 and the depolarization has an almost flat response over the entire spectra. Thus, it can be generalized that SC generated in any media at such high input powers has maximum depolarization.

The estimated peak power for the formation of stable single filament is ~ 26 MW (i.e., $\sim 10P_{cr}$) for the media considered here. As we increase the input power ($\sim 100P_{cr}$), we start observing multiple filament formation where the num-

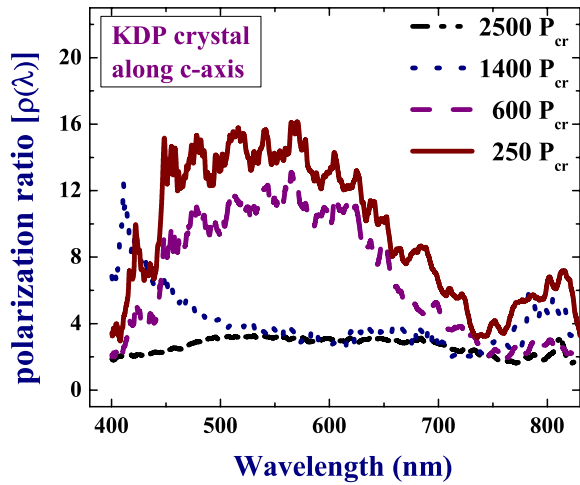


FIG. 6. (Color online) $\rho(\lambda)$ of the SC from KDP crystal along the c axis with an increase in the input power in terms of the critical power (P_{cr}).

ber of filaments increases sharply. Each of the individual filaments can generate white-light continuum [34]. The supercontinuum that is generated from each of these filaments possesses a high degree of spatial coherence, which has been demonstrated using a simple Young's double-slit configuration [21,35]. We start observing coherent interaction between the filaments leading to the fluctuating interference patterns in the far-field image of the output on a screen. At still higher powers (>270 MW, $\sim 100P_{cr}$), the number of filaments become very large with the effect that the intensity fluctuations within the profile of the beam almost diminish. When the filaments are more than one but are finite in number, the interference due to the filaments leads to a colored fringelike pattern within the beam profile. With a large number of filaments, these patterns merge leading to a uniform white continuum at every position of the beam cross section. The polarization of the continuum remains the same as the input polarization until the powers are raised to $\sim 100P_{cr}$, at which the number of filaments would be much higher than a single

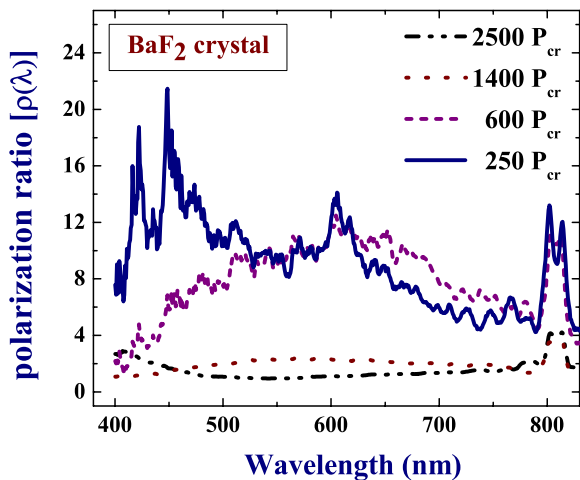


FIG. 7. (Color online) $\rho(\lambda)$ of the SC from BaF₂ crystal with an increase in the input power in terms of the critical power (P_{cr}).

filament. As mentioned earlier, although these filaments interfere and lead to multiple interference pattern across the beam cross section, we still observe that the polarization ratio is well maintained. Only at powers larger than $100P_{cr}$ does one start observing a drastic reduction in the polarization ratio. At such powers, we also expect the onset of plasma. This observation may indicate that the depolarization could be due to scattering by electron density inhomogeneities described by the dielectric tensor of the plasma [36] rather than due to multiple filamentation. Further studies need to be carried out to establish the reasons for the depolarization to quantify the contributions of plasma, multiple filamentation, and light scattering.

To conclude our observations up to now on the study of $\rho(\lambda)$ of the different media generating SC, we find the following: (a) the depolarization sets in the SC with an increase in input power, (b) different spectral components experience different depolarization with the wavelength band around the input fundamental peak getting maximum depolarization, (c) at higher input powers, the polarization is affected because of the combined effect of the interaction of pulse with plasma and the effect of the NAB. Thus, there is always a tradeoff between obtaining brighter SC at the cost of linear polarization properties of the SC. Any strategy to overcome this limitation would be of immense relevance to the growing demand of intense femtosecond white-light sources with better polarization properties.

B. Reduction of depolarization in KDP crystal

We find that amorphous isotropic media like BK-7 glass, which offers a better polarization ratio at low powers, does not hold any advantage at high input powers. Similarly, isotropic cubic media that are centrosymmetric, such as BaF₂, which has an intrinsic anisotropic $\chi^{(3)}$ tensor, cannot do any better at high input powers, although at low input powers there are recent reports on the anisotropic $\chi^{(3)}$ of cubic media being successfully used to control the onset of filamentation in a BaF₂ crystal [37] and to some extent getting a better polarization ratio in a CaF₂ crystal at a very low input power of $\sim 10P_{cr}$ [30]. However, KDP, being a noncentrosymmetric crystal, has an anisotropic $\chi^{(3)}$ tensor and hence the anisotropic nonlinear refraction (n_2) leads to nonlinear anisotropic birefringence (NAB) being different for different orientations of the crystal. Thus the magnitude of NAB depends strongly on the crystal orientation. Taking this cue, we carried out experiments to study the effect of orientation on $\rho(\lambda)$ in a KDP crystal. It should be noted here that the data shown upto now are for the SC generated along the c axis of the crystal through which the natural birefringence is not present ($n_o = n_e$) making it behave similar to an isotropic medium.

Since SCG is essentially a third-order process, it is intrinsically dependent on the $\chi^{(3)}$ of the material. The anisotropic property of the crystals results in dependence of $\chi^{(3)}$ on the rotation angle. The $\chi^{(3)}(\theta)$ is a function of the independent nonvanishing $\chi^{(3)}$ components determined by the symmetry. Isotropic cubic crystals like BaF₂ and CaF₂ having a space-group symmetry $43m$ have a well-defined expression for effective $\chi^{(3)}$ [38]. For uniaxial crystals, such as sapphire and

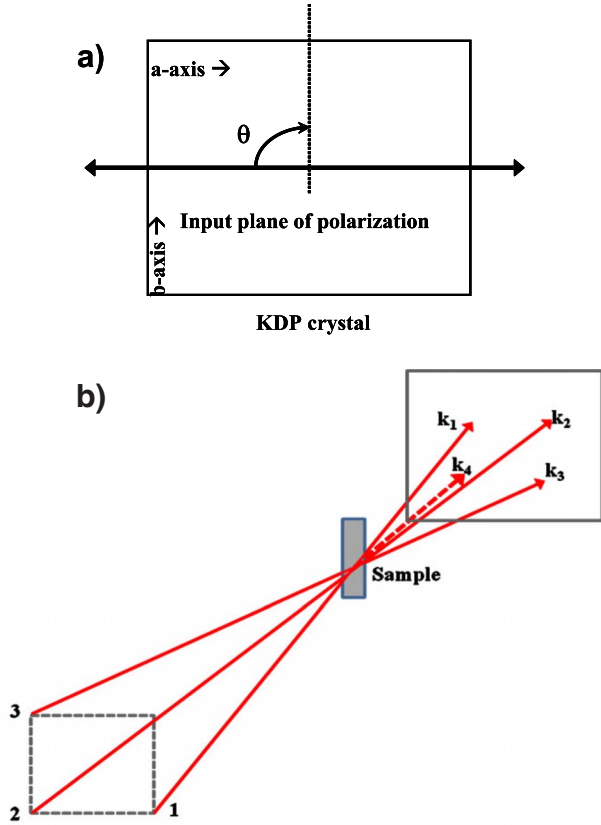


FIG. 8. (Color online) (a) Position of the crystal used for the DFWM study of the effect of orientation of plane of polarization relative to the horizontal polarization denoted by θ ; (b) geometry of the box-car DFWM setup.

KDP, the relation for effective $\chi^{(3)}$ becomes more complicated as there is a direction dependence for e rays but not for o rays [39]. Moreover, with KDP being noncentrosymmetric and having a tetragonal structure and $\bar{4}2m$ symmetry, the expression for effective $\chi^{(3)}$ is more complex [40].

In order to observe the dependence of effective $\chi^{(3)}$ with simple orientation of the crystal, we carried out degenerate four-wave mixing (DFWM) studies in forward box-car geometry [41] on a thin slice of the z -cut crystal by rotating the plane of polarization of the input laser beam with respect to the 0° position (i.e., horizontal polarization) rotated by a HW plate as shown in Fig. 8(a). In brief, in a box-car arrangement the fundamental beam is divided into three nearly equal intensity beams in such a way that the three form three corners of a square box and are focused into the nonlinear medium (sample) both spatially and temporally. The DFWM signal that comes as the fourth corner of the box was generated as a result of the phase-matched interaction $k_4 = k_3 - k_2 + k_1$ of the three incident beams, as shown in Fig. 8(b). The third-order nonlinear susceptibility $\chi^{(3)}$ is obtained by comparing the measured DFWM signal for the sample with that of fused silica as reference ($\chi^{(3)} = 1.4 \times 10^{-14}$ esu) under the same experimental conditions. The following relationship is used [41]:

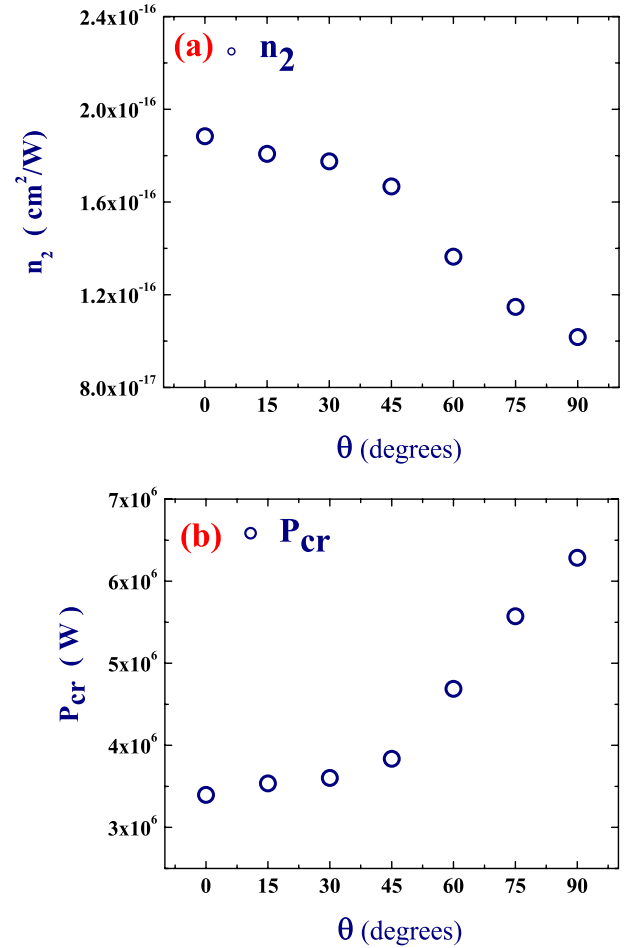


FIG. 9. (Color online) (a) Variation of n_2 with orientation of plane of input polarization relative to the horizontal polarization denoted by θ . (b) Variation of P_{cr} with θ .

$$\chi_{\text{sample}}^{(3)} \text{ (esu)} = \left(\frac{n_{\text{sample}}}{n_{\text{ref}}} \right)^2 \left(\frac{I_{\text{sample}}}{I_{\text{ref}}} \right)^{1/2} \left(\frac{L_{\text{ref}}}{L_{\text{sample}}} \right) \times \alpha L_{\text{sample}} \left(\frac{e^{\alpha L_{\text{sample}}/2}}{1 - e^{-\alpha L_{\text{sample}}}} \right) \chi_{\text{ref}}^{(3)} \text{ (esu)}, \quad (1)$$

where I is the DFWM signal intensity, α is the linear absorption coefficient, L is the sample path length, and n is the refractive index taken as 1.48 and 1.45 for KDP crystal and fused silica, respectively, at 800 nm. From the observed $\chi^{(3)}$, we estimated the value of nonlinear refractive index (n_2) which is related to third-order nonlinear susceptibility by the relation [41]

$$n_2 \text{ (cm}^2\text{/W)} = \frac{0.0395}{n_0^2} \chi^{(3)} \text{ (esu)}. \quad (2)$$

Figure 9(a) shows the variation of n_2 with respect to the rotation of the plane of polarization of the input beam clearly indicating the intrinsic anisotropic nonlinearity in the KDP crystal. Correspondingly, the critical power for self-focusing (P_{cr}) that is inversely proportional to n_2 [4] increases with an increase in the angle of rotation, as seen in Fig. 9(b). After ascertaining the intrinsic anisotropic nonlinearity, we carried

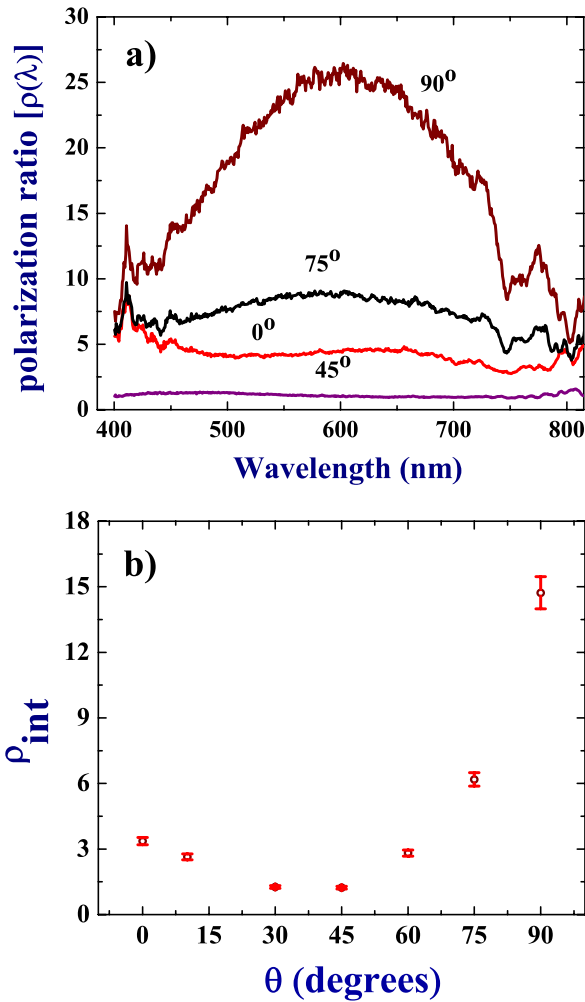


FIG. 10. (Color online) (a) $\rho(\lambda)$ for SCG obtained for different rotation of plane of input polarization; (b) variation of ρ_{int} with θ .

out polarization studies to investigate the effect of orientation of plane of polarization on $\rho(\lambda)$. Evidently, we see that the noncentrosymmetric KDP crystal can have orientation-dependent P_{cr} . Henceforth, in the latter part of this paper, the measurements are presented with respect the input peak intensity rather than in terms of the P_{cr} .

Figure 10(a) shows the variation of $\rho(\lambda)$ for the SC generated at an average input power of 350 mW that corresponds to a peak intensity of $\sim 8 \times 10^{12}$ W/cm² along the c axis of the crystal with rotation of the plane of input linear polarization. With rotation of the plane of polarization from 0° (horizontal) to 45° , we observed that the $\rho(\lambda)$ decreases and then increases from 45° to 90° . Clearly $\rho(\lambda)$ is at its minimum when the plane of polarization is rotated by 45° incidence, indicating that at this position $I_{\text{orth}}(\lambda)$ is almost equal to $I_{\text{par}}(\lambda)$ signifying maximum polarization degradation. However, upon rotation by 90° we have enhancement in the overall $\rho(\lambda)$ with an increase of polarization ratio in the wavelength region of 450–750 nm when compared to that obtained at 0° . Confirming the obtained spectral data, Fig. 10(b) shows the plot of variation of ρ_{int} as a function of rotation angle (θ). The presented data are the averaged values obtained by repeating the measurements three times with

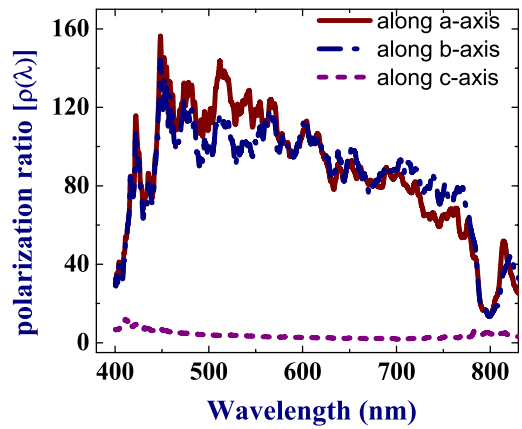


FIG. 11. (Color online) $\rho(\lambda)$ for SCG obtained for three axes of the crystal.

the error bars accounting for a possible 5% experimental error. In other words, with rotation of plane of input polarization, a better polarization ratio was obtained. We performed similar studies with BK-7 glass and BaF₂ crystal as well to see any change in the $\rho(\lambda)$. As expected, we did not see any alteration in the overall $\rho(\lambda)$, confirming that this is unique to an anisotropic medium like KDP crystal. However, a straightforward explanation to the observed dependence of the $\rho(\lambda)$ in KDP crystal is not possible with the available literature. Though we expect the $\rho(\lambda)$ to increase from 0° to 90° following a similar trend to the variation of P_{cr} , we observed a dip at 45° . The theoretical pursuit to understand this is still underway.

The $\rho(\lambda)$ for SC generated along the a , b , and c axis of the crystal for the same input power is as shown in Fig. 11. From the figure, it is evident that the SC along the a and b axes have a lower depolarization compared to that along the c axis, indicating most depolarization of SC along the c axis. $\rho(\lambda)$ is the lowest along the c axis probably because both the polarization components experience the same refractive index ($n_0 = n_e$). This led us to believe that SC along an axis other than the c axis should improve the polarization ratio. To confirm this assertion, we carried out our depolarization studies at orientations other than the principal coordinates. We rotated the crystal around the b axis with the zeroth position as the direction with the plane of polarization parallel to the a axis. Figure 12 shows that as we move away from the c axis, the spectral dependence of $\rho(\lambda)$ gets better when rotated by 30° relative to the zeroth position. Continuing along these lines, we generated SC along several other orientations of the crystal obtaining different $\rho(\lambda)$. At one such orientation determined to be along $\theta = 45^\circ$ and $\varphi = 3.5^\circ$ (where θ is the angle propagation vector relative to the c axis, and φ is the azimuth angle), the generated SC was found to be having the least depolarization. Figures 13(a) and 13(b) shows the SC output in parallel and perpendicular positions of the analyzer, respectively, for this orientation in comparison to that obtained along the c axis ($I_{\text{in}} \sim 8 \times 10^{12}$ W/cm²). On the left side of Fig. 13, we present the snapshot of the SC output at the two orthogonal positions of the analyzer. Clearly the contrast between SC outputs generated is large when generated along the preferred orientation

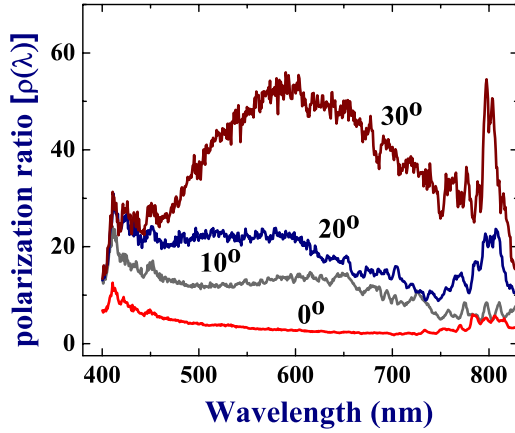


FIG. 12. (Color online) $\rho(\lambda)$ for SC generated at different crystal orientations (see text).

when compared to that when generated along the c axis. The right side of the figure shows the corresponding spectra obtained for the SC outputs at both the orthogonal positions of the analyzer. It is evident that along the preferred crystal orientation we did not obtain any spectral output when the analyzer is at the orthogonal position, in contrast to a comparable output when SC generated along the c axis. The integrated intensity measurements of the SC output with rotation of the analyzer is shown in Fig. 14. The output polarization has a maximum along the direction of the input plane of polarization and we do not observe any rotation in the plane of polarization. The measurements also indicate

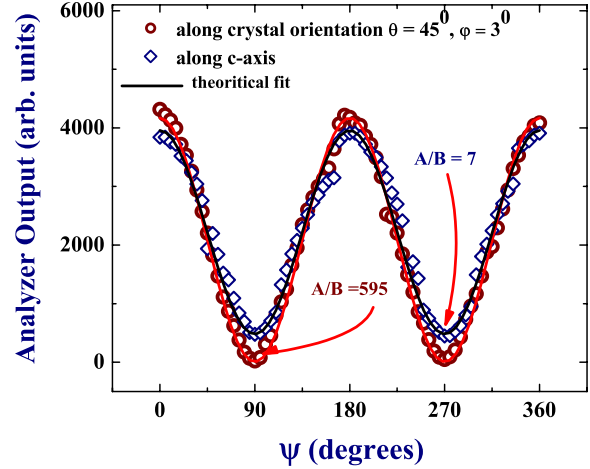


FIG. 14. (Color online) Plot of the analyzer output of the SC generated along specified orientation and the c axis of the KDP crystal with respect to the rotation of the analyzer.

that the SC is not elliptically polarized but gets partially depolarized. The solid curve shown in the figure is a theoretical fit obtained for the relation, $y = A \cos^2(\psi) + B \cos^2(90 - \psi)$, where ψ is the angle of rotation of the analyzer, A is the intensity parallel to the input plane of polarization, and B represents the depolarized component along the orthogonal direction. For SC generated along the c axis, we obtained A/B to be $\sim 7:1$ when compared to a high ratio of $\sim 595:1$ for SC generated along the preferred orientation of the KDP crystal.

Thus, we show that for a noncentrosymmetric crystal, the depolarization of the SC is dependent on the direction of propagation of the fundamental, and the depolarization can be conveniently reduced by choosing the specified direction of propagation. Figure 15 shows the plot of ρ_{int} obtained for SC along a particular direction with an increase in input peak intensity in comparison to what is already obtained for the generated SC along the c axis of the crystal. There was no observable signal in I_{orth} position for intensities below 1.2×10^{12} W/cm² in the case of the SCG at the specified orien-

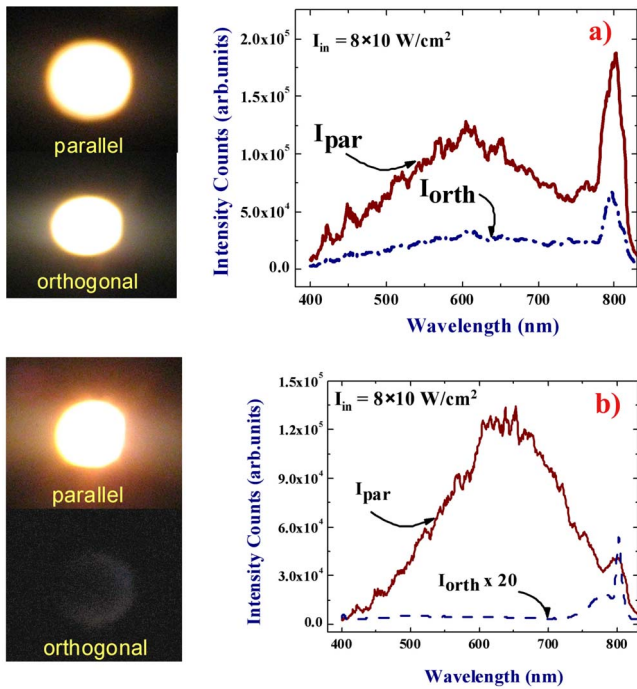


FIG. 13. (Color online) (left) Snapshot of the SCG at the parallel and orthogonal orientation of the analyzer; (right) the spectra recorded for SC at the corresponding analyzer position: (a) SC generated along the c axis of KDP; (b) SC generated along the preferred orientation of the crystal.

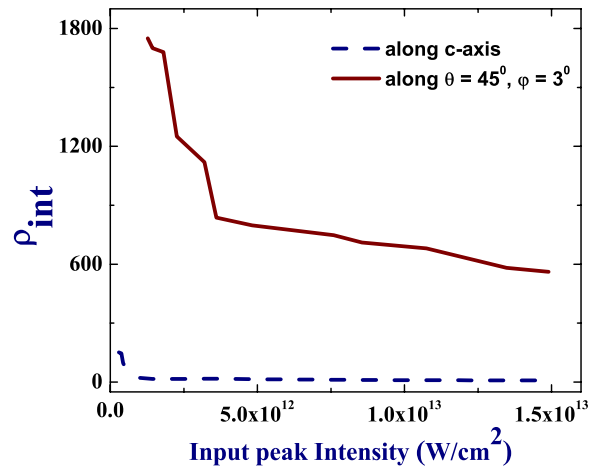


FIG. 15. (Color online) ρ_{int} of the KDP SC at different orientation with an increase in the input peak intensities.

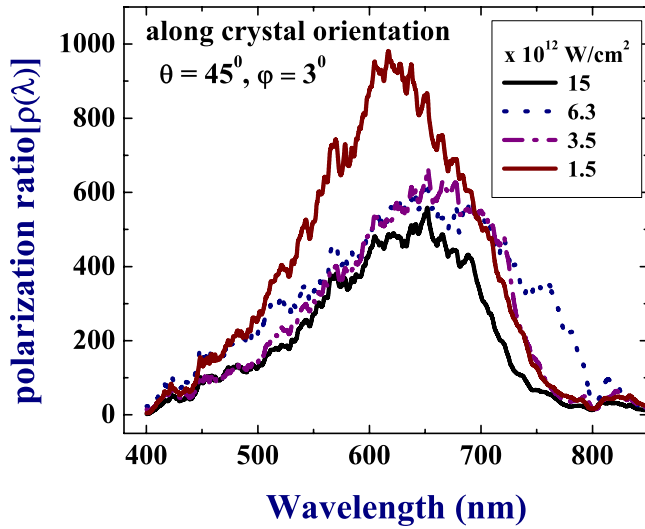


FIG. 16. (Color online) $\rho(\lambda)$ for SCG along the preferred crystal orientation for various input peak intensities.

tation of the crystal, which tells us that the ρ_{int} at lower intensities are much larger than 1800 and that there is no depolarization of SC. We observe that for input intensity beyond 1.5×10^{12} W/cm² (i.e., beyond $250P_{\text{cr}}$ for other media presented earlier) where other media experience the onset of depolarization, the SC in this case has less depolarization. For lower input intensities, we see that the ratio is much higher and comparable to what we measure for the input pulse. $\rho(\lambda)$ for SC generated at different input intensities is shown in Fig. 16. We find that even at high input intensities the spectral response of $\rho(\lambda)$ remains similar to what is obtained for lower input intensities. Although we did not attempt to study the polarization properties for input peak intensity more than 15×10^{12} W/cm², it is expected to have lower depolarization looking at the trend of variation of $\rho(\lambda)$ at higher input intensities.

In our earlier report, the coherence properties were proved to be well maintained even at higher input powers [21]. The control over polarization properties of SCG in KDP thus helps with well-defined polarization properties. To date the best reported ρ is 2000:1 for SCG in CaF₂ achieved at low input power $\sim 10P_{\text{cr}}$ with single filament generation [30]. Thus, the present results hold significance with SC being generated at much higher input peak powers and intensities, allowing intense SC generation with minimum depolarization. Though as shown earlier in this paper BK-7 glass had better $\rho(\lambda)$ compared to BaF₂ and *z*-cut KDP crystal, it fails to match the ratio obtained for SC generated along the pre-

ferred orientation of KDP crystal. Thus, this makes KDP crystal a better choice of media for generating SC for obtaining the best polarization properties. With its large band gap ~ 7.12 eV (174 nm) [42], high damage threshold, and strong nonlinear behavior allowing the enrichment of spectral content in the blue region by parametric wave-mixing [22], KDP acts as a versatile candidate for SCG. On the theoretical front, reports available in understanding the SCG aspect of propagation of ultrashort pulses in quadratic media are sporadic in nature. We expect our results, presented here, to encourage the much needed theoretical work.

IV. CONCLUSIONS

To conclude the present results in this paper, we have systematically studied the depolarization properties of the generated SC in different classes of media, namely (a) BK-7 glass representing isotropic amorphous condensed media, (b) BaF₂ isotropic crystalline condensed media, and (c) KDP crystal anisotropic crystalline condensed media. We carried out our work by studying the variation of the polarization ratio $[\rho(\lambda)]$ defined as $I_{\text{par}}(\lambda)/I_{\text{orth}}(\lambda)$ for SC obtained at different input powers for three media under consideration. We find that at low input powers, SC generated in BK-7 glass has better $\rho(\lambda)$, indicating minimum depolarization when compared to that in BaF₂ and KDP along its *c* axis. At high input powers, we observe that SC from all three media undergoes maximum depolarization with low $\rho(\lambda)$. As a strategy to obtain better $\rho(\lambda)$, the intrinsic noncentrosymmetric property of KDP crystal was used and we observed that $\rho(\lambda)$ of SCG depends strongly on the following: (i) the plane of polarization of incident light and (ii) the incident plane of the crystal. Though one would expect the polarization degradation of SCG at high input intensities, we observed a dramatic reduction in the depolarization with a change in orientation of the crystal with respect to the *c* axis of KDP. Our results show that the depolarization of SCG is most when generated along the *c* axis. It is anticipated that these conclusions that have diverse implications in applied areas will simulate enough interest in the research on a theoretical front, providing much required insight into the overall understanding of SCG in quadratic media.

ACKNOWLEDGMENTS

R.S.S.K. acknowledges the financial support of CSIR-SRF. The authors are grateful to Babu N. J. Reddy and Professor H. L. Bhatt, Department of Physics, IISc, Bangalore for lending the *z*-cut KDP crystal for this work. We also acknowledge the financial support of the Department of Science and Technology (DST), India.

[1] R. R. Alfano, *The Supercontinuum Laser Source* (Springer-Verlag, Berlin, 1989).
 [2] J. M. Dudley, G. Genty, and S. Coen, *Rev. Mod. Phys.* **78**, 1135 (2006).
 [3] N. Bloembergen, *Opt. Commun.* **8**, 285 (1973).
 [4] J. H. Marburger, *Prog. Quantum Electron.* **4**, 35 (1975).

[5] A. L. Gaeta, *Phys. Rev. Lett.* **84**, 3582 (2000).
 [6] A. Couairon, E. Gaižauskas, D. Faccio, A. Dubietis, and P. Di Trapani, *Phys. Rev. E* **73**, 016608 (2006).
 [7] H. Ward and L. Bergé, *Phys. Rev. Lett.* **90**, 053901 (2003).
 [8] N. Akozbek, M. Scalora, C. M. Bowden, and S. L. Chin, *Opt. Commun.* **191**, 353 (2001).

- [9] M. Kolesik, G. Katona, J. V. Moloney, and E. M. Wright, *Appl. Phys. B: Lasers Opt.* **77**, 185 (2003).
- [10] R. A. Negres and J. M. Hales, *IEEE J. Quantum Electron.* **38**, 1205 (2002).
- [11] B. Schenkel, R. Paschotta, and U. Keller, *J. Opt. Soc. Am. B* **22**, 687 (2005).
- [12] G. Cerullo and S. de Silvestri, *Rev. Sci. Instrum.* **74**, 1 (2003).
- [13] T. Udem, R. Holzwarth, and T. W. Hansch, *Appl. Phys. B* **416**, 233 (2002).
- [14] M. Balu, J. Hales, D. Hagan, and E. Van Stryland, *Opt. Express* **13**, 3594 (2005).
- [15] J. H. Frank, A. D. Elder, J. Swartling, A. R. Venkitaraman, A. D. Jeyasekharan, and C. F. Kaminski, *J. Microsc.* **227**, 203 (2007).
- [16] J. K. Ranka, R. S. Windeler, and A. J. Stentz, *Opt. Lett.* **25**, 25 (2000).
- [17] T. A. Birks, W. J. Wadsworth, and P. S. J. Russell, *Opt. Lett.* **25**, 1415 (2000).
- [18] S. Coen, A. H. L. Chau, R. Leonhardt, J. D. Harvey, J. C. Knight, W. J. Wadsworth, and P. S. J. Russell, *J. Opt. Soc. Am. B* **19**, 753 (2002).
- [19] A. K. Dharmadhikari, F. A. Rajgara, and D. Mathur, *Appl. Phys. B: Lasers Opt.* **80**, 61 (2005).
- [20] K. Wang, L. Qian, H. Luo, P. Yuan, and H. Zhu, *Opt. Express* **14**, 6366 (2006).
- [21] N. K. M. N. Srinivas, S. S. Harsha, and D. N. Rao, *Opt. Express* **13**, 3224 (2005).
- [22] R. S. S. Kumar, S. S. Harsha, and D. N. Rao, *Appl. Phys. B: Lasers Opt.* **86**, 615 (2007).
- [23] A. K. Dharmadhikari, F. A. Rajgara, and D. Mathur, *Opt. Lett.* **31**, 2184 (2006).
- [24] I. Buchvarov, A. Trifonov, and T. Fiebig, *Opt. Lett.* **32**, 1539 (2007).
- [25] P. Tzankov, I. Buchvarov, and T. Fiebig, *Opt. Commun.* **203**, 107 (2002).
- [26] M. Ziolk, R. Naskrecki, and J. Karolczak, *Opt. Commun.* **241**, 221 (2004).
- [27] K. Midorikawa, H. Kawano, A. Suda, C. Nagura, and M. Obara, *Appl. Phys. Lett.* **80**, 923 (2002).
- [28] A. Srivastava and D. Goswami, *Phys. Lett. A* **341**, 523 (2005).
- [29] I. Golub, *Opt. Lett.* **15**, 305 (1990).
- [30] V. Kartazhev and R. R. Alfano, *Opt. Commun.* **281**, 463 (2008).
- [31] R. S. S. Kumar, K. L. N. Deepak, and D. N. Rao, *Opt. Lett.* **33**, 1198 (2008).
- [32] A. L'Huillier, Ph. Balcou, S. Candel, K. J. Schafer, and K. C. Kulander, *Phys. Rev. A* **46**, 2778 (1992).
- [33] J. Yang, N. Zhang, and X. Zhu, *Appl. Phys. B: Lasers Opt.* **89**, 261 (2007).
- [34] R. G. Brewer, J. R. Lifshitz, E. Garmire, R. Y. Chiao, and C. H. Townes, *Phys. Rev.* **166**, 326 (1968).
- [35] K. Cook, A. K. Kar, and R. A. Lamb, *Appl. Phys. Lett.* **83**, 3861 (2003).
- [36] R. W. Boyd, *Nonlinear Optics*, 2nd ed. (Elsevier, Amsterdam, 2003).
- [37] A. K. Dharmadhikari, K. Alti, J. A. Dharmadhikari, and D. Mathur, *Phys. Rev. A* **76**, 033811 (2007).
- [38] R. Adair, L. L. Chase, and S. A. Payne, *Phys. Rev. B* **39**, 3337 (1989).
- [39] Q. Guo and S. Chi, *J. Opt. A, Pure Appl. Opt.* **2**, 5 (2000).
- [40] I. A. Kulagin, R. A. Ganeev, R. I. Tugushev, A. I. Rysanyan-sky, and T. Usmanov, *J. Opt. Soc. Am. B* **23**, 75 (2006).
- [41] R. L. Sutherland, *Handbook of Nonlinear Optics* (Dekker, New York, 1996).
- [42] G. Dimitriev, G. G. Gurzadyan, and D. N. Nikogosyan, *Handbook of Nonlinear Optical Crystals*, 2nd revised ed. (Springer, Berlin, 1977).